

Supplementary Materials
for
**VEGF Receptor Inhibitors Block The Ability of Metronomically Dosed
Cyclophosphamide To Activate Innate Immunity-Induced Tumor Regression**

Joshua C. Doloff and David J. Waxman

Department of Biology
Boston University
5 Cummington Street
Boston, MA 02215 USA

Contents:

Supplementary Materials and Methods

Supplementary Figure Legends

Supplementary Tables S1, S2

Supplementary Figures S1-S4

Supplementary Materials and Methods

Reagents - CPA was purchased from Sigma Chemical Co. (St. Louis, MO). The VEGF receptor inhibitors axitinib (AG-013736) and AG-028682 were provided by Pfizer (New York, NY). Cediranib (AZD2171) was purchased from Selleck Chemicals LLC (cat. #S1017). Fetal bovine serum (FBS) and DMEM were purchased from Invitrogen (Frederick, MD).

qPCR analysis - Total RNA was isolated from frozen tumor or spleen tissue using TRIzol (Invitrogen; Carlsbad, CA) according to the manufacturer's instructions. Reverse transcription of 1 µg total RNA in a volume of 20 µl was carried out using the High Capacity cDNA Reverse Transcription kit (Cat. #4368814; Applied Biosystems, Foster City, CA). cDNA (4.8 µl; 1:50 dilution) in a total vol of 16 µl (including SYBR Green and PCR primers) was amplified by qPCR using primers shown in Supplemental Table S1. Primers were designed using Primer Express software (Applied Biosystems, Carlsbad, CA, USA) and analyzed using LaserGene software (DNASar, Madison, WI, USA) to ensure mouse-specificity. The absence of cross-species amplification was verified by testing each primer set on a panel comprised of rat liver, human HUVEC cell, and mouse liver RNAs in addition to rat 9L and human U251 tumor cell RNAs. Samples were incubated at 95°C for 10 min followed by 40 cycles of 95°C for 15 sec and 60°C for 1 min in an ABI PRISM 7900HT Sequence Detection System (Applied Biosystems). Results were analyzed using the comparative C_T method as described by the manufacturer. Data are presented as relative level of each RNA compared to the RNA level in untreated tumors after normalization to the 18S RNA content of each sample. In qPCR comparisons of gene expression in nod-scid-gamma (NSG) and scid mice shown in Fig. 5, C_T values determined by qPCR (i.e., log₂ values that indicate relative levels of gene expression for untreated tumor and spleen samples) between NSG and *scid* models, respectively, were as follows: NKp46 (Tumors: >40 and 29; Spleens: 34.2 and 23.8); NK1.1 (Tumors: 34.5 and 31.9; Spleens: 34 and 27.3); GzmB (Tumors: >40 and 31.6; Spleens: 33.3 and 28); Prf1 (Tumors: >40 and 34.6; Spleens: >40 and 28.7); and CD68 (Tumors: 22.3 and 22.4; Spleens: 23.4 and 21.8).

FACS analysis – Single-cell suspensions of freshly excised tumor tissue were prepared using a gentleMACS Dissociator (Miltenyi Biotec, Auburn, CA) according to the manufacturer's protocol for implanted tumors. Tumor single-cell suspensions (5 ml) were diluted to 15 ml with PEB dissociation buffer (1 x PBS, pH 7.2, 0.5% BSA, and 2 mM EDTA), passed through a 70 µm filter (cat. #22363548, Fisher Scientific) and then subjected to red blood cell lysis with 5 ml 1X RBC lysis buffer (cat. #00-4333, eBioscience, San Diego) for 5 min at room temperature. The reaction was terminated by the addition of 20 ml of sterile 1 x PBS. The cells remaining were centrifuged at 300-400g at 4°C and resuspended in minimal (~50 µl) eBioscience Staining Buffer for antibody incubation. Samples were incubated in the dark for 25 min at 4°C with a fluorescently tagged monoclonal antibody specific for the NK cell marker NK1.1 (1 µl (0.5 µg) per sample, FITC-NK1.1, clone PK136, cat. #11-5941, eBioscience). Background samples were similarly stained with FITC-labeled Rat IgG (1 µl per sample, cat. #553929, eBioscience). eBioscience Flow Cytometry Staining Buffer (2 ml; cat. #00-4222, eBioscience) was then added, and the samples were centrifuged at 400-500 g for 5 min at 4°C. Supernatants were removed by aspiration, and this wash step was repeated two more times with staining buffer. Following the third wash, each sample was resuspended in 500 µl of Flow Cytometry Staining Buffer and passed through a 40 µm filter (cat. #22363547, Fisher Scientific) for FACS analysis using a BD FACSCalibur instrument (cat. #342975; BD Biosciences).

Tissue processing and immunohistochemistry – Tumors were collected on day 0 (first day of drug treatment) and on various days after initiating drug treatment. Generally, for U251 tumors, samples were collected six days after the first, second, and third cycles of metronomic CPA treatment, corresponding to days 6, 12, and 18 after initiating drug treatment. GL261 and 9L tumors were collected on day 0, and six days after the second, fourth, and seventh cycles of metronomic CPA, i.e., days 12, 24, and 42, as indicated in each Figure. Tumors were excised and portions were then frozen in liquid nitrogen (for RNA preparation) or in 2-methylbutane (for tissue sectioning and immunohistochemistry). Cryosections (5-10 μ m) were prepared and fixed in 4% paraformaldehyde (for CD68 immunostaining) or acetone (for NK1.1 and CD74 immunostaining). Slides were stained using rat anti-mouse mAb CD68 antibody (Clone FA-11, cat. #MCA1957, Ab Serotec, Raleigh, NC, USA) at a dilution of 1:50, goat anti-mouse NK1.1 (CD161) antibody (Clone M-15, cat. #sc-70150, Santa Cruz Biotech, Santa Cruz, CA, USA) at a dilution of 1:25, rat anti-mouse mAb CD74 (Clone ln-1, cat. #sc-19627, Santa Cruz Biotech) at a dilution of 1:50, or rat anti-mouse CD31 (Cat. #557355, BD Biosciences Pharmingen, San Jose, CA) at a dilution of 1:1000. An avidin-biotin blocking kit (cat. #SP-2001, Vector Labs, Burlingame, CA, USA) was used for all incubations. Finally, a biotinylated rabbit anti-rat (cat. #BA-4000) or rabbit anti-goat (cat. #BA-5000) secondary antibody was used at a dilution of 1:250, followed by ABC signal amplification with Vectastain ABC peroxidase reagent (cat. #PK-4000), and then VIP (cat. #SK-4600) or DAB (cat. #SK-4100) (all from Vector labs) detection reagent.

Image acquisition and analysis – Stained tumor sections were visualized under an Olympus BX51 microscope. Tiled images covering 5-20 sections were collected (depending on tumor size) for at least two regions within at least two tumors for each treatment group and time point analyzed. Images were captured with an Olympus DP25 digital camera using Olympus DP2-BSW software. For stain quantification, images were converted into 8-bit image files, a background threshold was determined using NIH ImageJ, and all images were then processed using an NIH ImageJ macro to quantify the area of positive stain. Data shown are group average values \pm S.E. Statistically significant differences between mean values of different treatment groups were determined by two-tailed Student's t-tests; *, $p < 0.05$; **, $p < 0.001$; and ***, $p < 0.0001$.

Supplementary Figure Legends

Figure S1, related to Figure 1. Correlation between host (m, mouse) PEDF and TSP1 RNA levels across large sets of individual 9L (A) and U251 (B) tumors. Tumors were grown s.c. in *scid* mice and collected at various times after the initiation of metronomic CPA treatment, in the presence or absence of axitinib treatment, as shown for U251 tumors in Figure 1A. A strong correlation was seen in both tumor models ($r = 0.89$), as determined by qPCR analysis using gene-specific primers shown in Table S1 (see Supplemental Materials). $n = 60$ individual tumors for both panels A and B. Individual RNA samples from each treatment group are shown as follows: UT tumors, red; Ax-treated tumors, blue; metronomic CPA-treated tumors, green; and metronomic CPA + Ax treatment, purple.

Figure S2, related to Figure 2. Additional markers of innate immune cell responses to metronomic CPA and axitinib treatment. Innate immune cell marker responses to metronomic CPA (140 mg/kg, every 6 days, i.p.), \pm axitinib (Ax), as indicated, in 9L or U251 brain tumor xenografts grown in *scid* mice. Metronomic CPA increased the expression of: (A) macrophage markers CD68 and F4/80 (Emr1); (B) macrophage cytolytic effectors lysozyme 1 and lysozyme 2 (Lyz1 and Lyz2); (C) natural killer cell marker NK1.1; and (D) dendritic cell marker CD74, in both 9L (left) and U251 (right) tumors. All three factors were suppressed by axitinib given daily for 24 days (9L tumors) or daily from day 0 until 6 days after the 2nd or 3rd CPA treatment (U251 tumors), as indicated. Bars, mean \pm SE for $n = 5-6$ tumors/group.

Figure S3, related to Figure 2. Further analysis of innate immune cell responses to metronomic CPA and axitinib.

(A) Representative immunostaining images of macrophage marker CD68 (*left*), NK cell marker NK1.1 (*middle*), and dendritic cell marker CD74 (*right*) in untreated U251 tumors (*no Rx*) or in U251 tumors treated with metronomic CPA \pm axitinib, as in Figure 1A, and isolated from *scid* mice on treatment day 12. 1st row of images, untreated tumors (*No Rx*); 2nd row, metronomic CPA treated (*CPA*); and 3rd row, metronomic CPA + axitinib (*CPA+Ax*). Images shown are representative and have signal intensities equivalent to the group mean, based on ImageJ quantification.

(B) NIH ImageJ quantification of CD68 (*left*), NK1.1 (*middle*), and CD74 (*right*) immunohistochemical staining. Data shown are % positive area values, and were determined using images taken at the same magnification; thus, they are all expected to be directly comparable to each other, and indicate the relative extent of tumor infiltration by each innate immune cell subtype. **: $p < 0.001$; ***: $p < 0.0001$ for the comparisons indicated. See “Experimental Procedures” for details on quantification of immunohistochemical signals.

(C) *Top*, qPCR analysis of granzyme (Gzm) A (*left*) and GzmC (*right*) RNA levels in the same U251 tumors analyzed in Figure S2, *right*. Axitinib blocked the induction of granzyme A by metronomic CPA and suppressed the basal level of granzyme C. *Bottom*, qPCR analysis of GzmB (*left*), GzmC (*middle*), and perforin (Prf1) (*right*) expression in the same 9L tumors analyzed in Figure S2, *left*. Bars, mean \pm SE for $n = 5-6$ tumors/group.

(D) FACS analysis showing increase in NK1.1⁺ cell population in 9L tumor xenografts after 2 and 4 cycles of metronomic CPA treatment. Percentages shown indicate the NK1.1⁺ cell fraction of the

total in the indicated 9L tumor single-cell suspensions. CD49b, which showed no change, was the marker used along the x-axis.

Figure S4, related to Figure 5. qPCR characterization of innate and adaptive immune markers in metronomic CPA-treated GL261 tumors in perforin knock-out/C57BL/6 mice, taken 6 days after the 4th CPA treatment cycle.

(A) While perforin knock-out impaired cytotoxic lymphocyte (NK, NKT, and T cell) activity leading to the initial impairment and eventual loss of metronomic CPA-induced tumor regression, as in Fig. 6A, innate and adaptive immune cells were still recruited to the metronomic CPA-treated GL261 tumors, as seen here in the comparisons to day 0 untreated (UT) controls. Data are shown for n=4 individual tumors in each group. Genes assayed include: NK cell marker NKp46, NK cell marker NK1.1 (also a potential NKT marker), macrophage marker CD68, dendritic cell marker CD74, and cytotoxic T cell marker CD8, as marked. C_T values (i.e., log₂ expression levels) for untreated tumor and spleen samples were: NK1.1: 28.7 and 25.1; NKp46: 28.4 and 24.5; CD68: 19.6 and 17; and CD74: 22 and 21.3, respectively. Full-length perforin transcripts were not detectable compared to no reverse transcriptase controls when assayed using qPCR primers flanking the functional knockout neomycin cassette insertion in exon 3. Less complete regression was observed as compared to wild-type responses (both with and without NK-depleting anti-asialo-GM1 antibody treatment), as observed in Fig. 6A. Thus, while NK cells are crucial for complete regression, NKTs and cytotoxic T cells may also contribute to metronomic CPA-induced tumor regression.

(B) Expression of immune markers in tumors (*left*) and spleens (*right*) isolated from two different mouse strains (C57BL/6 vs. *scid*) and tumor models (GL261 vs. 9L). Immune markers were assayed by qPCR analysis of tumors and spleens of untreated and metronomic CPA-treated C57BL/6 mice bearing GL261 tumors, and *scid* mice bearing 9L tumors, as indicated at the bottom. Tumors and spleens were isolated at the indicated time points and were analyzed in parallel by qPCR for natural killer cell markers NKp46 and NK1.1, cytotoxic effector granzyme B (GzmB), pore-forming perforin (Prf1), and macrophage marker CD68. C_T values for untreated tumor and spleen samples between the C57BL/6 and *scid* models, respectively: NKp46 (Tumors: 28.3 and 29; Spleens: 24.3 and 23.8); NK1.1 (Tumors: 28.6 and 31.9; Spleens: 25.1 and 27.3); GzmB (Tumors: 26.9 and 31.6; Spleens: 27 and 28); Prf1 (Tumors: 30.9 and 34.6; Spleens: 27.7 and 28.7); and CD68 (Tumors: 23 and 22.4; Spleens: 21.9 and 21.8). Data shown for *scid*-derived tumors and spleens is the same as represented in the vs. NSG comparison in Fig. 5C. The C57BL/6 samples were also processed in parallel and are thus directly comparable between this figure and the data shown in Fig. 5C. As in Fig. 5C, for each comparison, the first untreated (UT) *scid* tumor or spleen sample bar was normalized to 1. White and shaded bars indicated untreated and drug-treated samples, respectively. Bars, mean \pm SD for tumor (n=4-6) and spleen (n=2-3) pools.

Supplementary Tables

Table S1 – Regression of GL261 gliomas in response to metronomic CPA treatment. GL261 tumors grown in wild type (WT) C57BL/6 mice were treated with metronomic CPA (140 mg/kg BW, every 6 days) alone or in combination with the NK-depleting antibody anti-asialo-GM1, as shown in Fig. 6A. GL261 tumors were also grown and treated with metronomic CPA in C57BL/6-Prf1⁻ (perforin knock-out) mice. Data shown are mean \pm SD values for n = 12 tumors/group and are calculated from the data graphed in Fig. 6A. N/A, not applicable, as complete regression was not achieved.

Mouse Strain	Drug Treatment	No. of days until onset of tumor regression (from start of CPA treatment)	Days to 50% volume decrease (after onset of tumor regression)	Days to complete GL261 regression (from start of CPA treatment)	No. of completely regressed tumors
WT C57BL/6	metronomic CPA	3.8 \pm 1.4	7.0 \pm 2.2	39.6 \pm 16.2	12/12
WT C57BL/6	metronomic CPA + GM1	13.2 \pm 2***	16.1 \pm 3.3***	N/A	0/12
C57BL/6-Prf1 ⁻ (no perforin)	metronomic CPA	16.3 \pm 3***, ##	15.7 \pm 3.2*** or >42 days ^a	N/A	0/12

^a - 4 of 12 GL261 tumors treated with metronomic CPA in perforin knock-out mice never regressed to 50% of their maximal volume, after 42-51 days of monitoring.

***, p < 0.0001, as compared to WT (CPA alone), two-tailed Student's t-test.

##, p < 0.001, as compared to WT (CPA+GM1), two-tailed Student's t-test.

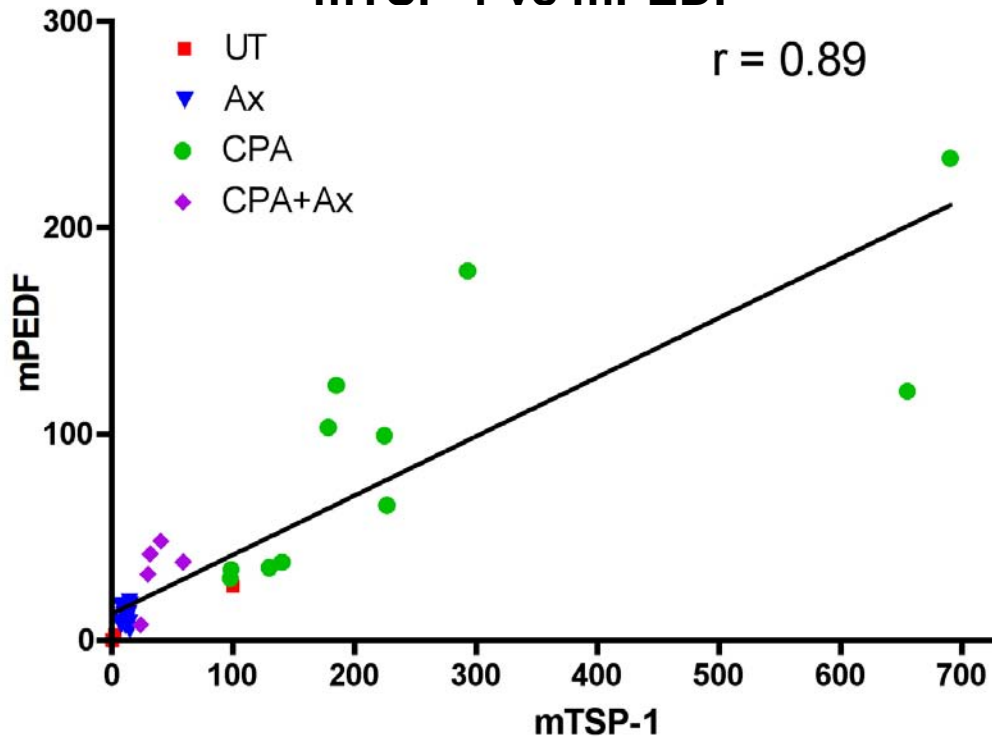
Table S2 – Forward and reverse primer sets used for qPCR analysis of the indicated RNAs. All primers were designed to amplify mouse sequences, but not the corresponding human or rat sequences, with the exception of MICB, which is human specific. Mouse specificity was achieved by designing primers to anneal at their 3' end only to mouse sequences. Species alignments between human, rat, and mouse sequences were used for each gene to determine primer set specificity. The absence of cross-species amplification was verified by testing primer sets on a panel of rat, mouse, and human RNAs to ensure species-specificity, as described above. Gene names are shown in parenthesis.

Gene	Oligo number	Primers (5' to 3'): Sense & Antisense
Thrombospondin-1 (TSP-1, <i>Thbs1</i>)	1459	Forward: 5'-TGTTCAAGAGGACCGGGCT-3'
	1460	Reverse: 5'-TGGATGGGTACATCCAGCTCC-3'
Pigment Epithelium-derived Factor (PEDF, <i>Serpinf1</i>)	3319	Forward: 5'-ACGGCCCTCTCTGCCCTTTCT-3'
	3320	Reverse: 5'-CTGTGGATGTCAGGGTTGGTGATCAG-3'
PECAM-1 (CD31, <i>Pecam1</i>)	1561	Forward: 5'-CCTCAGTCGGCAGACAAGATG-3'
	1562	Reverse: 5'-GCATAGAGCACCAGCGTGAGT-3'
Macrophage marker CD68 (<i>Cd68</i>)	3427	Forward: 5'-GCCCGAGTACAGTCTACCTGG-3'
	3428	Reverse: 5'-AGAGATGAATTCTGCGCCAT-3'
Lysozyme 1 (<i>Lyz1</i>)	5145	Forward: 5'-GATGGCTACCGTGGTGTCAA-3'
	5146	Reverse: 5'-AGCTCGTGTGTTATAATTGCTCTCA-3'
Lysozyme 2 (<i>Lyz2</i>)	5147	Forward: 5'-GTGCAAAGAGGGTGGTGAGA-3'
	5148	Reverse: 5'-CAGATCTCGGTTTTGACAGTGTG-3'
Macrophage marker F4/80 (<i>Emr1</i>)	3975	Forward: 5'-GATACAGCAATGCCAAGCAGT-3'
	3976	Reverse: 5'-TTGTGAAGGTAGCATTACAAGTGTA-3'
Fas receptor (<i>Fas</i>)	3100	Forward: 5'-ATCGCCTATGGTTGTTGACCA-3'
	3101	Reverse: 5'-AGATTTGAGGCATTCATTGGTATG-3'
iNOS (<i>Nos2</i>)	3359	Forward: 5'-TCTGCAGCACTTGGATCAGG-3'
	3360	Reverse: 5'-TTCGGAAGGGAGCAATGCCC-3'
Arginase-1 (<i>Arg1</i>)	3361	Forward: 5'-GCAAGGTGATGGAAGAGACCT-3'
	3362	Reverse: 5'-GACATCAAAGCTCAGGTGAATC-3'
Natural Killer Cell Factor 1.1 (NK1.1, <i>Klrb1c</i>)	3435	Forward: 5'-GCTGTGCTGGGCTCATCCT-3'
	3436	Reverse: 5'-TTGATGGTTTTTGTACTAAGACTCGCA-3'
NKp46 (<i>Ncr1</i>)	4668	Forward: 5'-GCAACCCCCTGAAACTGGTA-3'
	4669	Reverse: 5'-AAGGTTACCTCAGGCTGTGGATA-3'
Granzyme A (<i>GzmA</i>)	3559	Forward: 5'-GACTGCTGCCCACTGTAACG-3'
	3560	Reverse: 5'-TCAATATCTGTTGTTCTGGCTCCTTA-3'
Granzyme B (<i>GzmB</i>)	3561	Forward: 5'-TGTCTCTGGCCTCCAGGACAA-3'
	3562	Reverse: 5'-CTCAGGCTGCTGATCCTTGATCGA-3'

Granzyme C (<i>GzmC</i>)	3563	Forward: 5'-CCCCATCCAGACTATAATCCTGATG-3'
	3564	Reverse: 5'-CACAGCTCTAGTCCTCTTGGCAT-3'
Perforin (<i>Prfl</i>)	3565	Forward: 5'-GTACAACTTTAATAGCGACACAGTA-3'
	3566	Reverse: 5'-AGTCAAGGTGGAGTGGAGGT-3'
CD74 (<i>Cd74</i>)	3385	Forward: 5'-CCCAGGACCATGTGATGCAT-3'
	3386	Reverse: 5'-CTTAAGATGCTTCAGATTCTCT-3'
Langerin (<i>Cd207</i>)	3722	Forward: 5'-GGACTACAGAACAGCTTGGAGAATG-3'
	3723	Reverse: 5'-TACTTCCAGCCTCGAGCCAC-3'
DC-SIGN (<i>Cd209</i>)	3726	Forward: 5'-AGGTGCTCTTCCTAGCTGTTTGGT-3'
	3727	Reverse: 5'-TTCCTGAGAACTGGGTATTTTGTAG-3'
Cytokine Interleukin-12beta (<i>IL-12β</i>)	3594	Forward: 5'-TTGAACTGGCGTTGGAAGCACG-3'
	3595	Reverse: 5'-GTGAGTTCTTCAAAGGCTTCAT-3'
Chemokine CXCL14 (<i>Cxcl14</i>)	3598	Forward: 5'-GCTTCATCAAGTGGTACAAT-3'
	3599	Reverse: 5'-CTGGCCTGGAGTTTTTCTTTCCAT-3'
Platelet Factor 4 (<i>Cxcl4, Pf4</i>)	3822	Forward: 5'-TGCTTCTGGGCCTGTTGTTT-3'
	3823	Reverse: 5'-TAAGATCTCCATCGCTTTCTTCG-3'
Neutrophil marker Ly6g (<i>Gr1, Ly6g</i>)	3830	Forward: 5'-TGCCCCTTCTCTGATGGATT-3'
	3831	Reverse: 5'-TGCTCTTGACTTTGCTTCTGTGA-3'
NK cell receptor NKG2D (<i>Klrk1</i>)	4433	Forward: 5'- TATCATAAGAGGAAGATACCCTATAGAAA-3'
	4434	Reverse: 5'-GTGTAAAGGGTGAATCGAATTGC-3'
NKG2D activating ligand (human) MICB (<i>MICB</i>)	4437	Forward: 5'-CTGTTTCTGGCCGTCGCCTT-3'
	4438	Reverse: 5'-GATCCATCCTGGGACAGCAC-3'
T-cell marker CD4 (<i>Cd4</i>)	4255	Forward: 5'-GAAGATTCTGGGGCAGCATGGCAAAG-3'
	4256	Reverse: 5'-TTTGGAAATCAAACGATCAA-3'
Cytotoxic T-cell effector marker CD8 (<i>Cd8a</i>)	4257	Forward: 5'-CTGCGTGGCCCTTCTGCTGTCCT-3'
	4258	Reverse: 5'-GGGACATTTGCAAACACGCT-3'
Treg marker FoxP3 (<i>Foxp3</i>)	4253	Forward: 5'-GCCTTCAGACGAGACTTGGAA-3'
	4254	Reverse: 5'-CTGGCCTAGGGTTGGGCATT-3'
B-cell marker CD19 (<i>Cd19</i>)	4259	Forward: 5'-GGAAACCTGACCATCGAGAG-3'
	4260	Reverse: 5'-TGGGACTATCCATCCACCAGTT-3'
Perforin(neo) (<i>Prfl</i> KO)	5143	Forward: 5'-GTCAGGCCAGCATAAGAGTAGCCA-3'
	5144	Reverse: 5'-AATGGGCCAAGCCCCTCTGT-3'

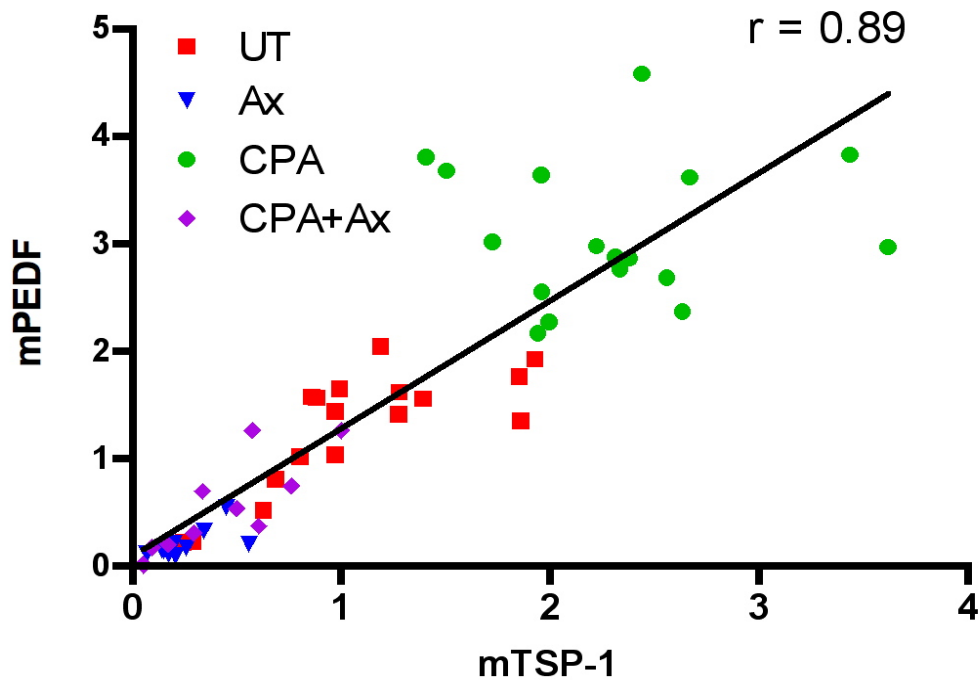
A. 9L:

mTSP-1 vs mPEDF



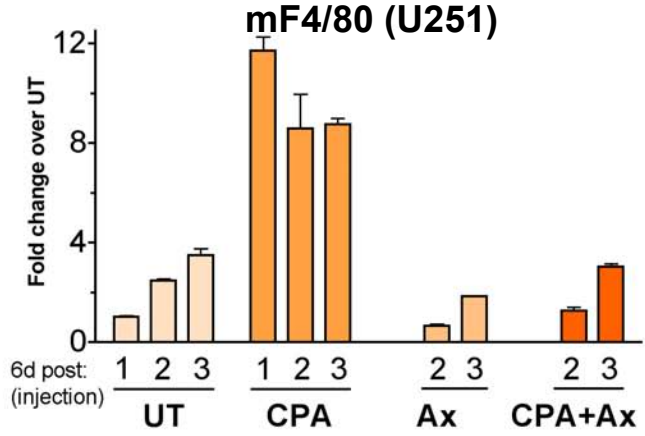
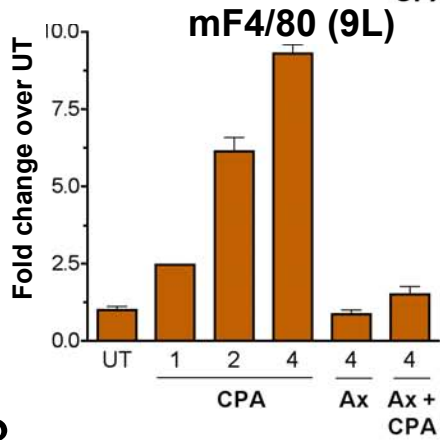
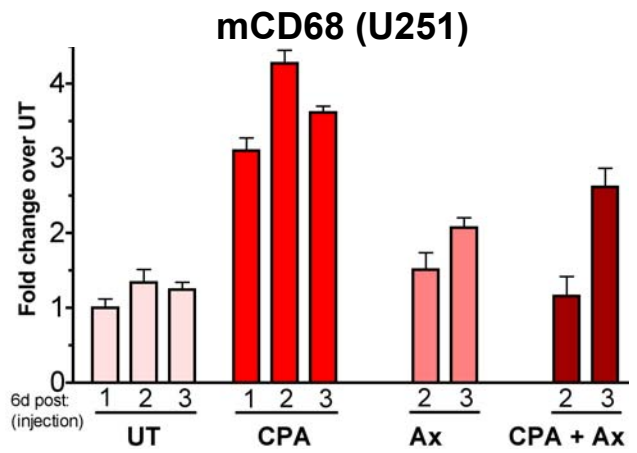
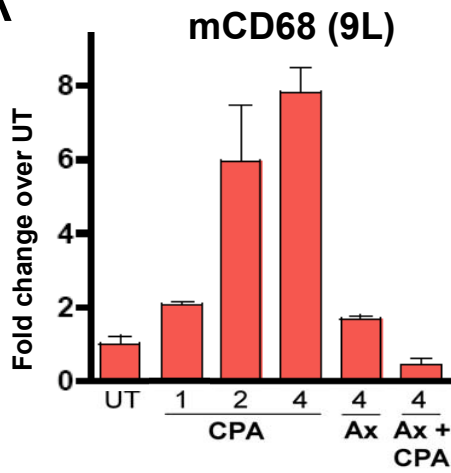
B. U251:

mTSP-1 vs mPEDF

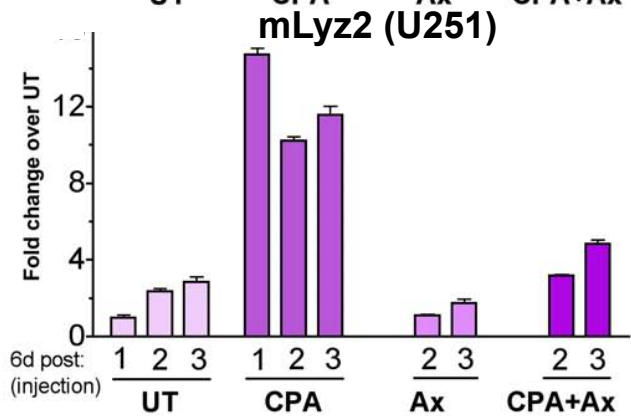
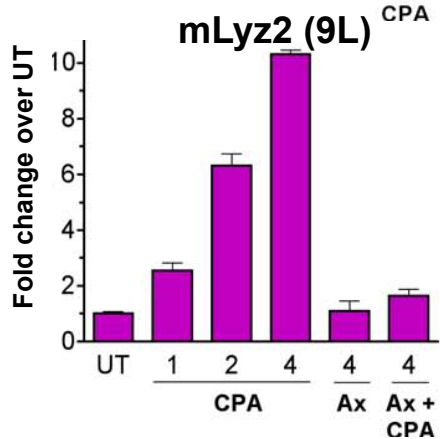
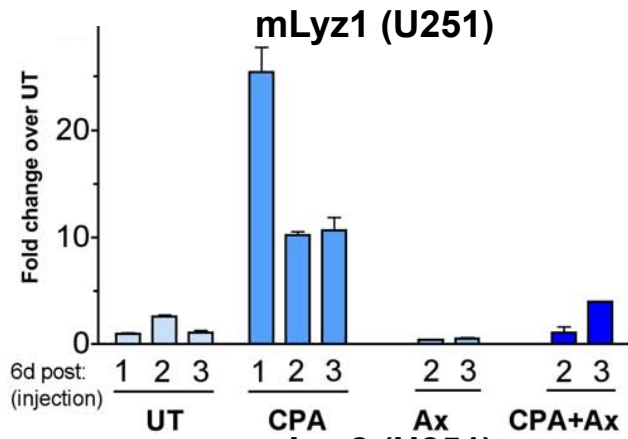
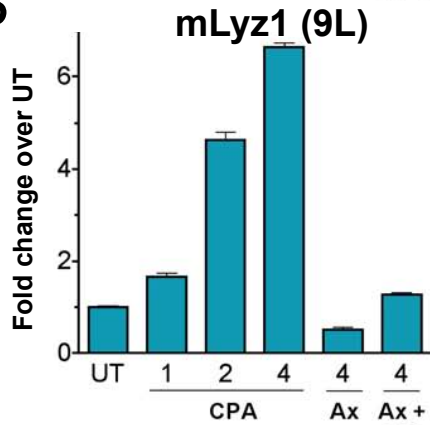


Supplemental Fig. S2A-B

A

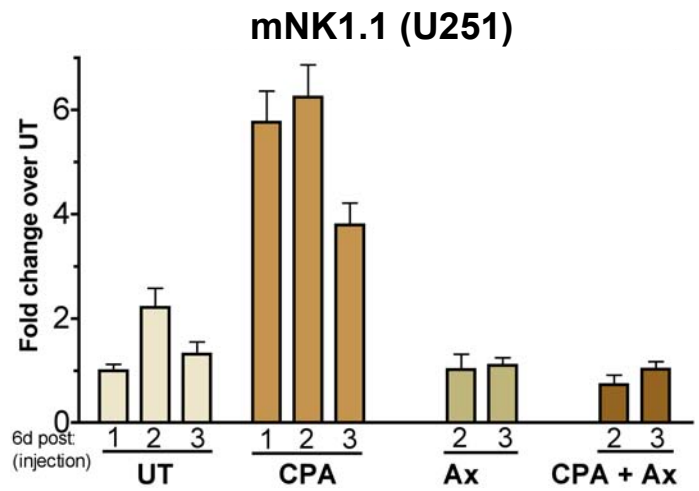
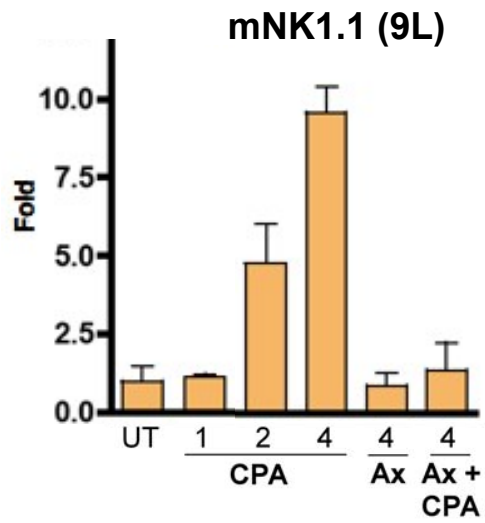


B

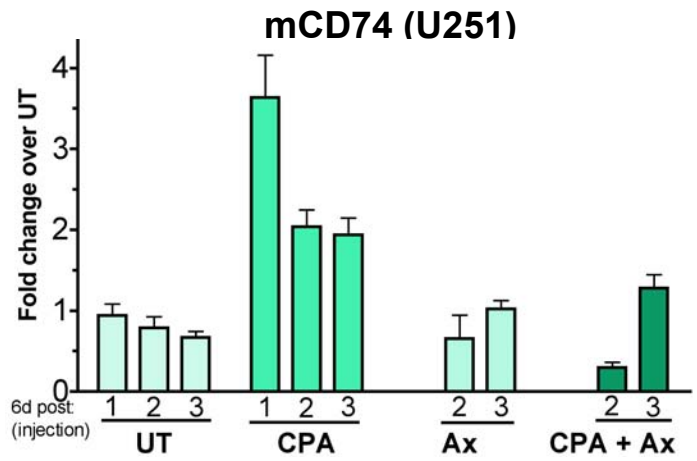
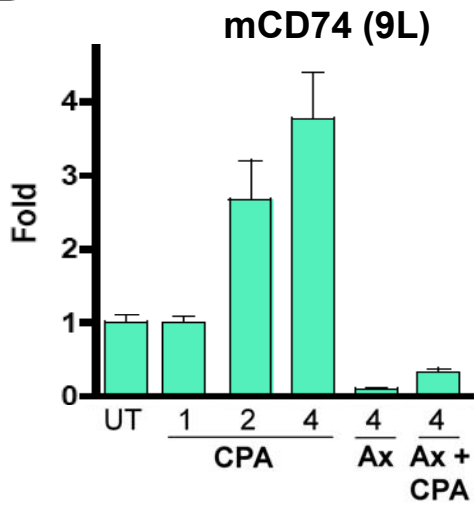


Supplemental Fig. S2C-D

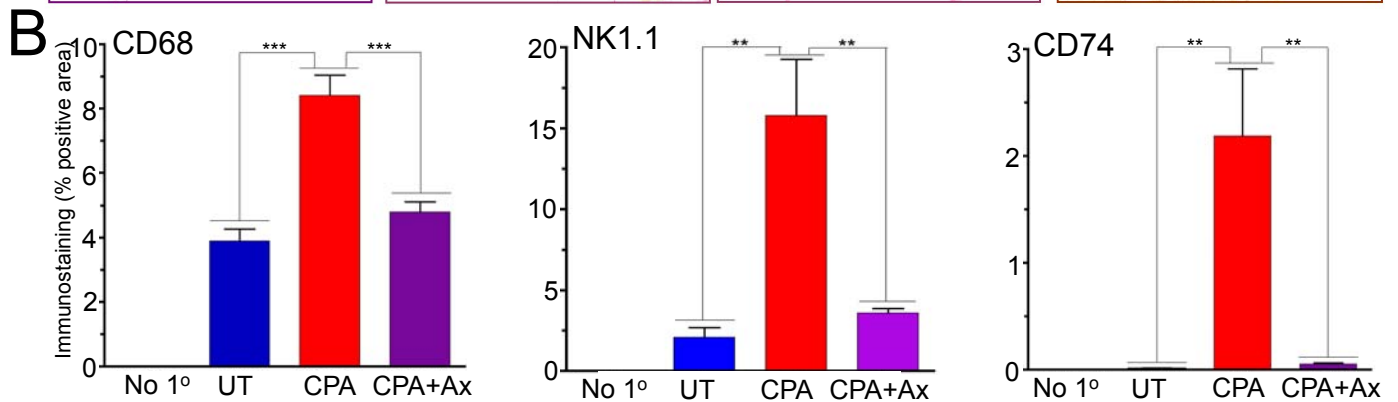
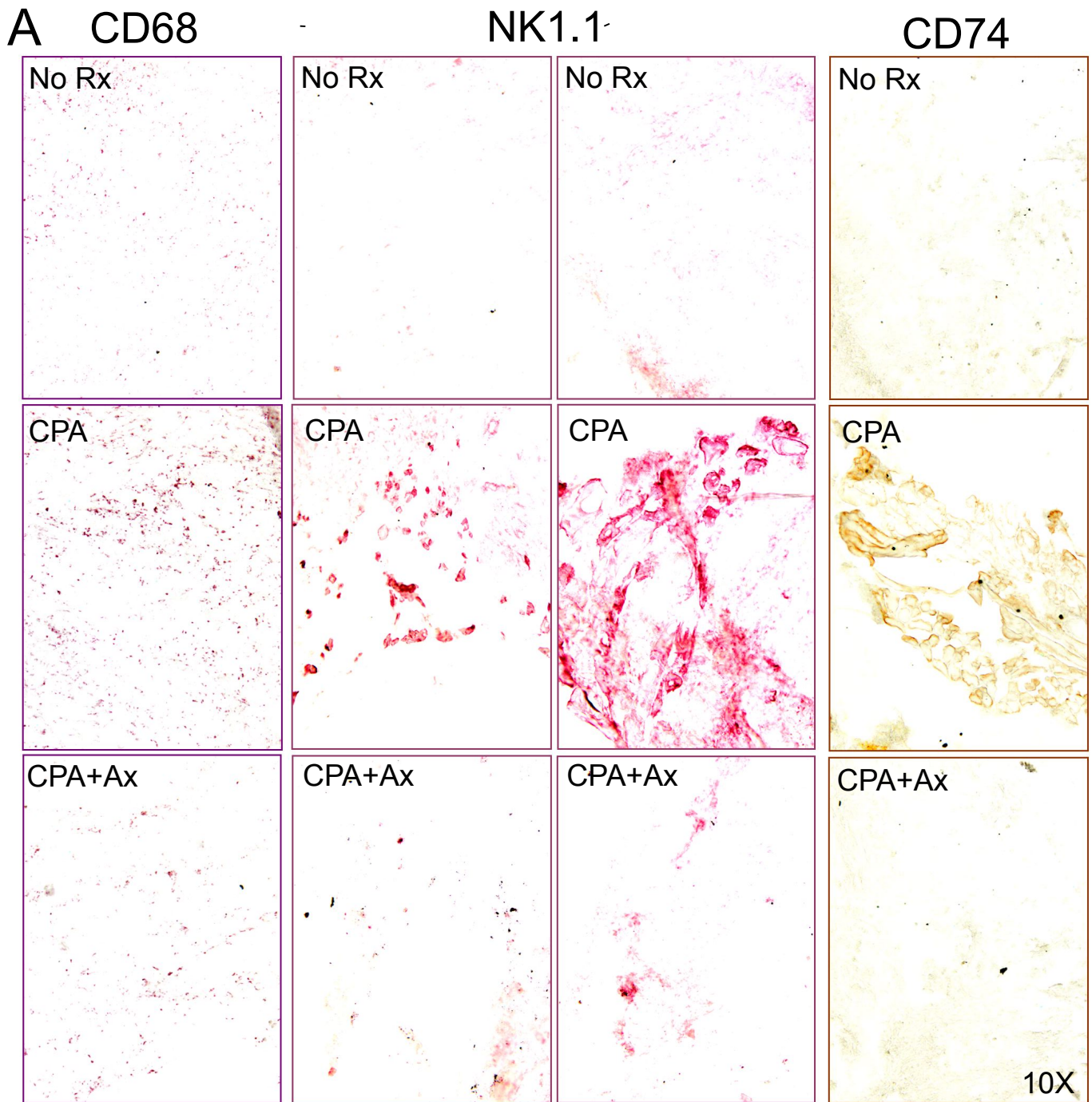
C



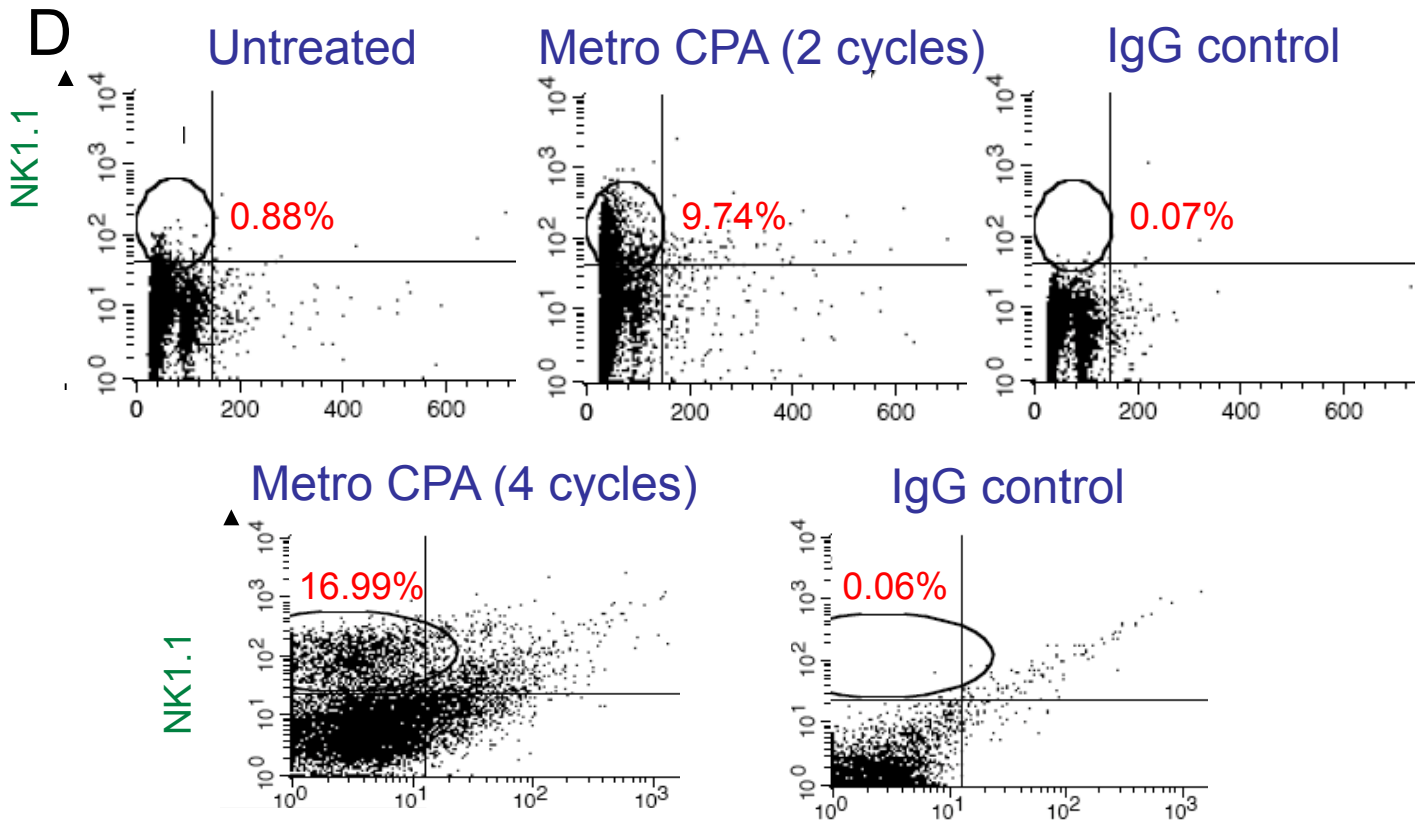
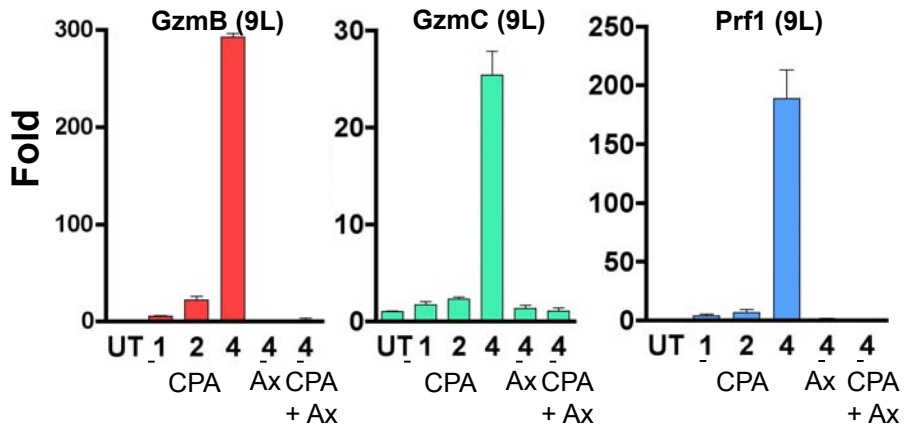
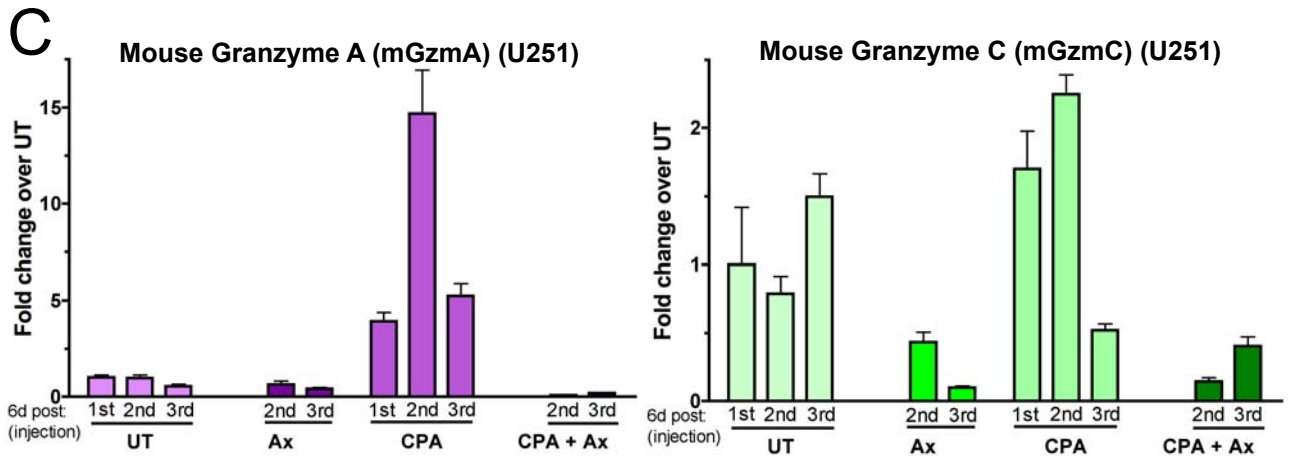
D



Supplemental Fig. S3A-B

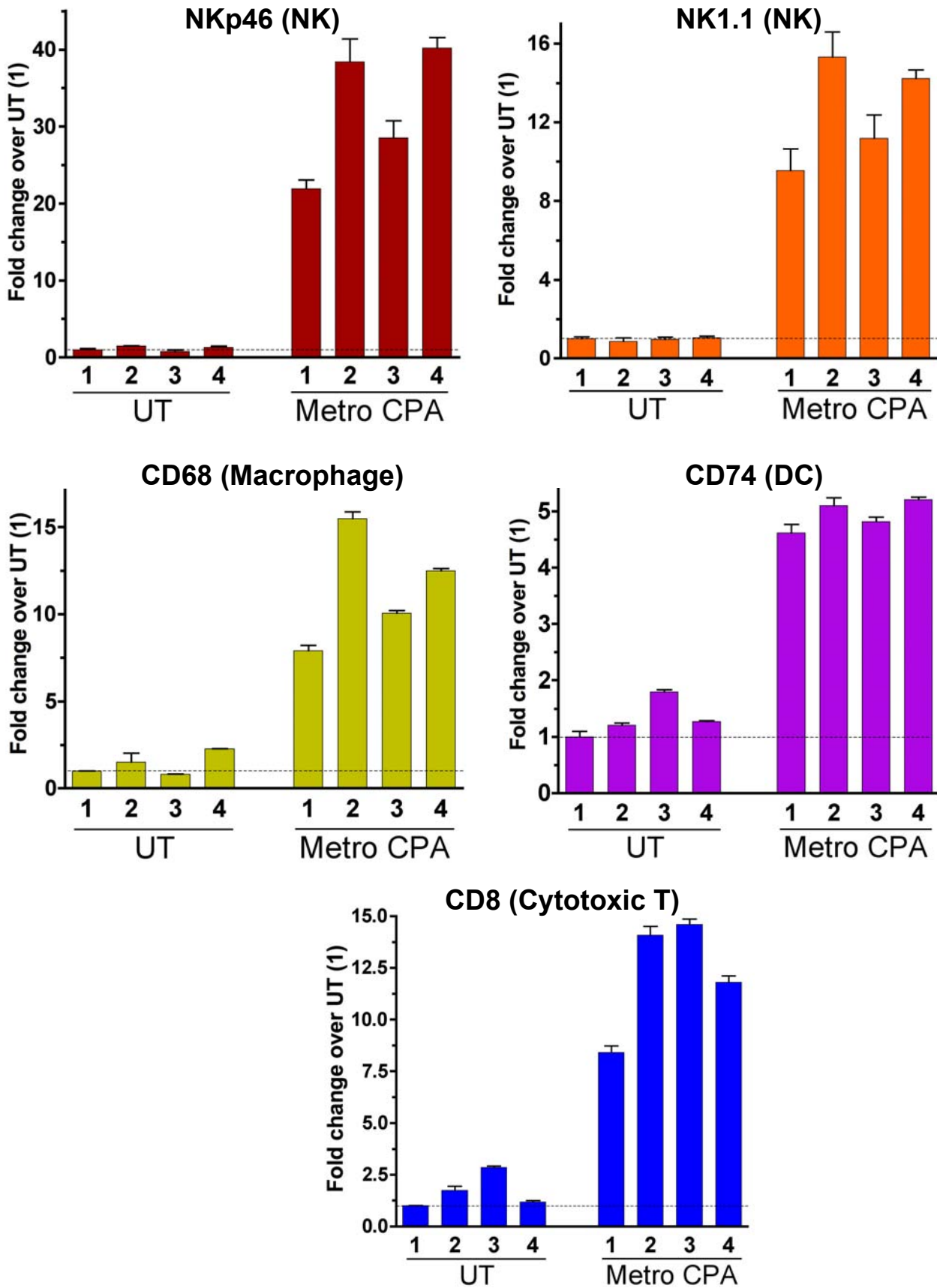


Supplemental Fig. S3C-D



Supplemental Fig. S4A

A, Prf1 KO:



Supplemental Fig. S4B

B

